Volume 15
Number 11
November 2024
Pages 3627–3914

RSC Medicinal Chemistry

rsc.li/medchem

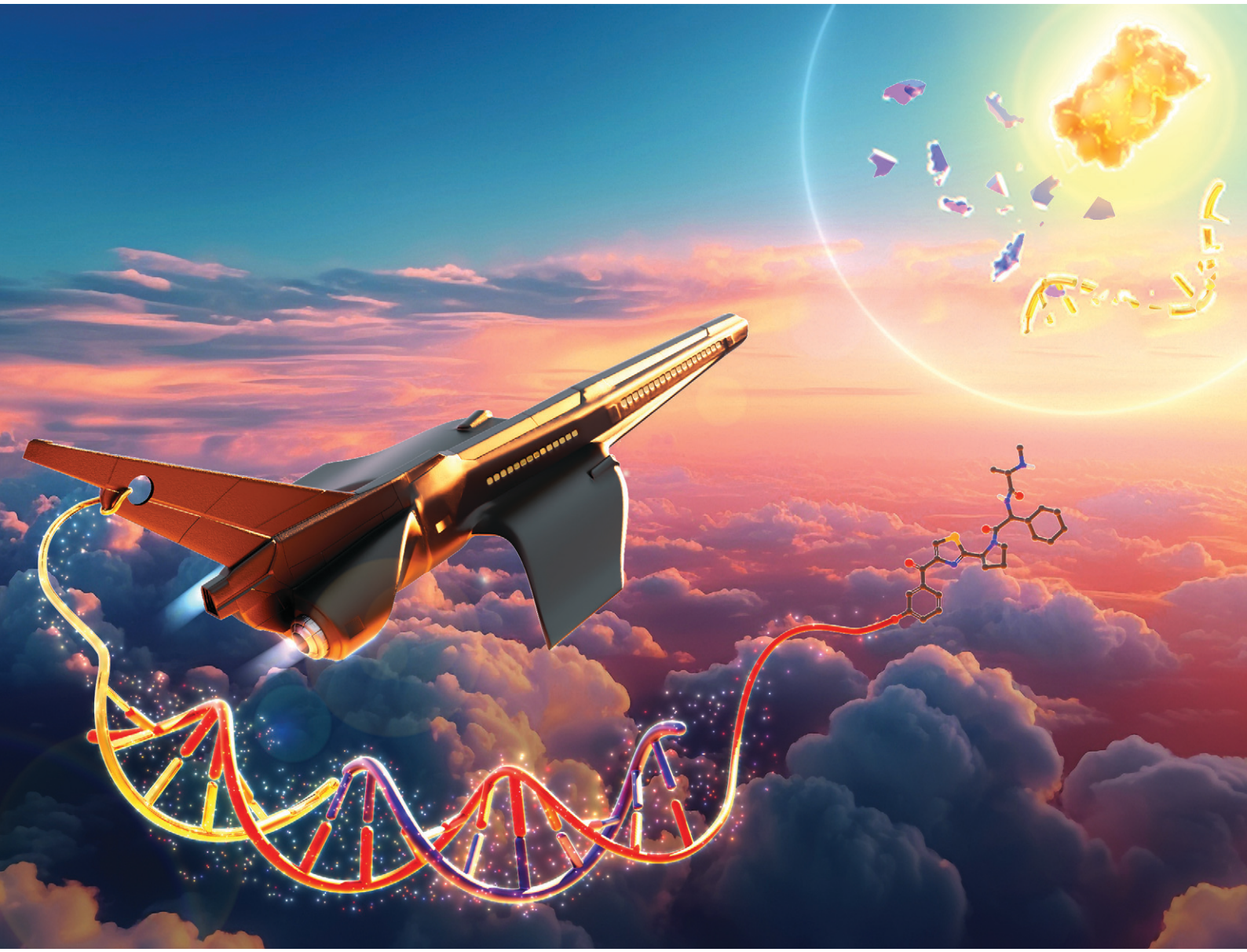

ISSN 2632-8682

ROYAL SOCIETY OF CHEMISTRY

RESEARCH ARTICLE
Nobumichi Ohoka, Yosuke Demizu *et al.*
Hydrophobic CPP/HDO conjugates: a new frontier in oligonucleotide-warheaded PROTAC delivery

RSC Medicinal Chemistry

ROYAL SOCIETY OF CHEMISTRY

RESEARCH ARTICLE

View Article Online
View Journal | View Issue

Check for updates

Cite this: *RSC Med. Chem.*, 2024, **15**, 3695

Hydrophobic CPP/HDO conjugates: a new frontier in oligonucleotide-warheaded PROTAC delivery†

Miyako Naganuma,[ab] Nobumichi Ohoka,*[c] Motoharu Hirano,[ab] Daishi Watanabe,[ab] Genichiro Tsuji,[a] Takao Inoue[c] and Yosuke Demizu*[abd]

Received 16th July 2024,
Accepted 22nd September 2024

DOI: 10.1039/d4md00546e

rsc.li/medchem

Proteolysis-targeting chimeras (PROTACs) have emerged as a potent strategy for inducing targeted degradation of proteins, offering promising therapeutic potential to treat diseases such as cancer. However, oligonucleotide-based PROTACs face significant delivery challenges because of their anionic nature and chemical instability. To address these issues, we developed a novel hydrophobic cell-penetrating peptide (CPP) and heteroduplex oligonucleotide (HDO)-conjugated PROTAC, **CPP/HDO-PROTAC**, to enhance intracellular delivery and degradation efficiency. **CPP/HDO-PROTAC** was designed to enter the cell through the activity of the conjugated hydrophobic CPP and release decoy oligonucleotide-based PROTACs by RNase H-mediated RNA strand breaks. Our findings demonstrated that **CPP/HDO-PROTAC** binds to the estrogen receptor α (ERα) with higher affinity than previous constructs, significantly degrades ERα in MCF-7 human breast cancer cells and inhibits cell proliferation at 10 μM. This research highlights the potential of **CPP/HDO-PROTAC** as a viable method for delivering and activating decoy oligonucleotide-based PROTACs within cells, overcoming the limitations of traditional transfection methods and paving the way for their clinical application.

Published on 05 1403. Downloaded on 23/09/1404 10:43:09 ..

1. Introduction

Over the past two decades, proteolysis-targeting chimeras (PROTACs) have become a potent strategy for addressing severe illnesses such as cancer.[1] These molecules induce the targeted destruction of proteins through the ubiquitin-proteasome system, showing versatility by targeting non-enzymatic proteins, including transcription factors (TFs) and scaffold proteins.[2] Building on the success of small molecule and peptide PROTACs designed for specific proteins, recent advances have generated decoy oligonucleotide-based PROTACs capable of targeting a wide range of TFs.[3] In 2021, Wei *et al.* reported a decoy oligonucleotide-based PROTAC targeting the TFs NF-κB and E2F, **TF-PROTAC**.[4] In the same year, an oligonucleotide PROTAC (**O′-PROTAC**), developed by Huang *et al.*, was shown to degrade LEF1 and ERG and reported to be effective *in vivo*.[5] In addition to decoy oligonucleotide-based PROTAC, several PROTACs using aptamers as warheads have been reported.[3,6–9] We previously reported decoy oligonucleotide-based PROTACs targeting estrogen receptor α (ERα), introducing PROTACs that combine three E3 ligase ligands — LCL161 for inhibitor of apoptosis protein (IAP), VH032 for von Hippel–Lindau and pomalidomide for cereblon.[10,11] Each variant (**LCL-ER(dec)**, **VH-ER(dec)** and **POM-ER(dec)**) efficiently degraded ERα. In addition, we have modified decoy oligonucleotides to enhance the chemical stability of PROTAC. Our findings revealed that this modified PROTAC, incorporating a standard nucleic acid modification, is more resistant to nucleases and maintains ERα-degrading activity longer than its unmodified counterpart.[11] Thus, in recent years, the development of several decoy oligonucleotide-based PROTACs has underscored their potential utility.[2,3] However, the delivery of oligonucleotide-based PROTACs to the plasma membrane poses challenges because of their low chemical stability with native sequences and their anionic properties, which complicate transport. In addition, the delivery of all reported oligonucleotide-based PROTACs into cells necessitates the use of transfection reagents, presenting a significant obstacle in their clinical deployment.

[a] *Division of Organic Chemistry, National Institute of Health Sciences, Kanagawa, Japan. E-mail: demizu@nihs.go.jp; Fax: +81 44 270 6578; Tel: +81 44 270 6578*
[b] *Graduate School of Medical Life Science, Yokohama City University, Kanagawa, Japan*
[c] *Division of Molecular Target and Gene Therapy Products, National Institute of Health Sciences, Kanagawa, Japan. E-mail: n-ohoka@nihs.go.jp; Tel: +81 44 270 6537*
[d] *Graduate School of Medicine, Dentistry and Pharmaceutical Sciences, Division of Pharmaceutical Science of Okayama University, Japan*

† Electronic supplementary information (ESI) available: The synthetic procedures for all compounds listed in this manuscript and the protocols for the *in vitro* assays (binding and protein degradation assays) (PDF). See DOI: **https://doi.org/10.1039/d4md00546e**

Published on 05 1403. Downloaded on 23/09/1404 10:43:09 ..

Nucleic acid therapeutics are gaining attention for their high therapeutic efficacy and specificity; however, efficient delivery poses a significant challenge. Developments in drug delivery systems (DDS) for these drugs, including antisense oligonucleotides (ASOs) and small interfering RNA (siRNA), aim to overcome this challenge and facilitate their practical application.[12,13] In particular, it has been reported that double-stranded RNA has a lower tissue distribution and cellular uptake efficiency than single-stranded ASO. Therefore, strategies for siRNAs include formulation with polymers or lipid nanoparticles[14] and binding to targeting ligands, including ligands for lipids and cell surface receptors. Although single-stranded ASOs can distribute to tissues and enter cells without special formulations or targeting ligands, reaching target mRNAs efficiently remains challenging. Ligand-conjugated ASOs have been explored to address this issue. Yokota *et al.* introduced heteroduplex oligonucleotides (HDOs) in 2015, comprising a DNA/LNA gapmer paired with its complementary RNA, enhanced by α-tocopherol as a DDS unit.[12,15] This configuration increased the activity of the gapmer-type ASO over single-stranded ASOs significantly by facilitating lipid release from the oligonucleotides for targeted mRNA delivery.

In this study, we introduced a cell-penetrating peptide (CPP) and heteroduplex oligonucleotide (HDO)-conjugated PROTAC (**CPP/HDO-PROTAC**) strategy, applying an CPP/HDO to enhance the delivery of a decoy oligoncleotide-based PROTAC into cells. This innovation enabled successful intracellular delivery and degradation of the target protein ERα, eliminating the need for transfection reagents. The **CPP/HDO-PROTAC**, a novel molecule, combines a 30-mer DNA linked to an LCL161 derivative (**LCL-HDO-F**) and a 30-mer DNA with a 9-mer RNA (**P4-HDO-R**) attached to a hydrophobic CPP (Fig. 1A and B). This design allows the **CPP/HDO-PROTAC** to enter cells *via* the hydrophobic CPP, **P4** peptide (LGAQSNF), and the potential release of the decoy oligonucleotide-based PROTAC through RNase H-mediated RNA strand cleavage and CPP detachment. The **P4** peptide was discovered through screening a 7-mer phage display peptide library for Duchenne muscular dystrophy treatment, aiming to deliver ASOs to targeted tissues.[16–19] Given the aggregation problems posed by the anionic nature of oligonucleotides when combined with cationic CPPs, the strategy shifted towards employing CPPs made of

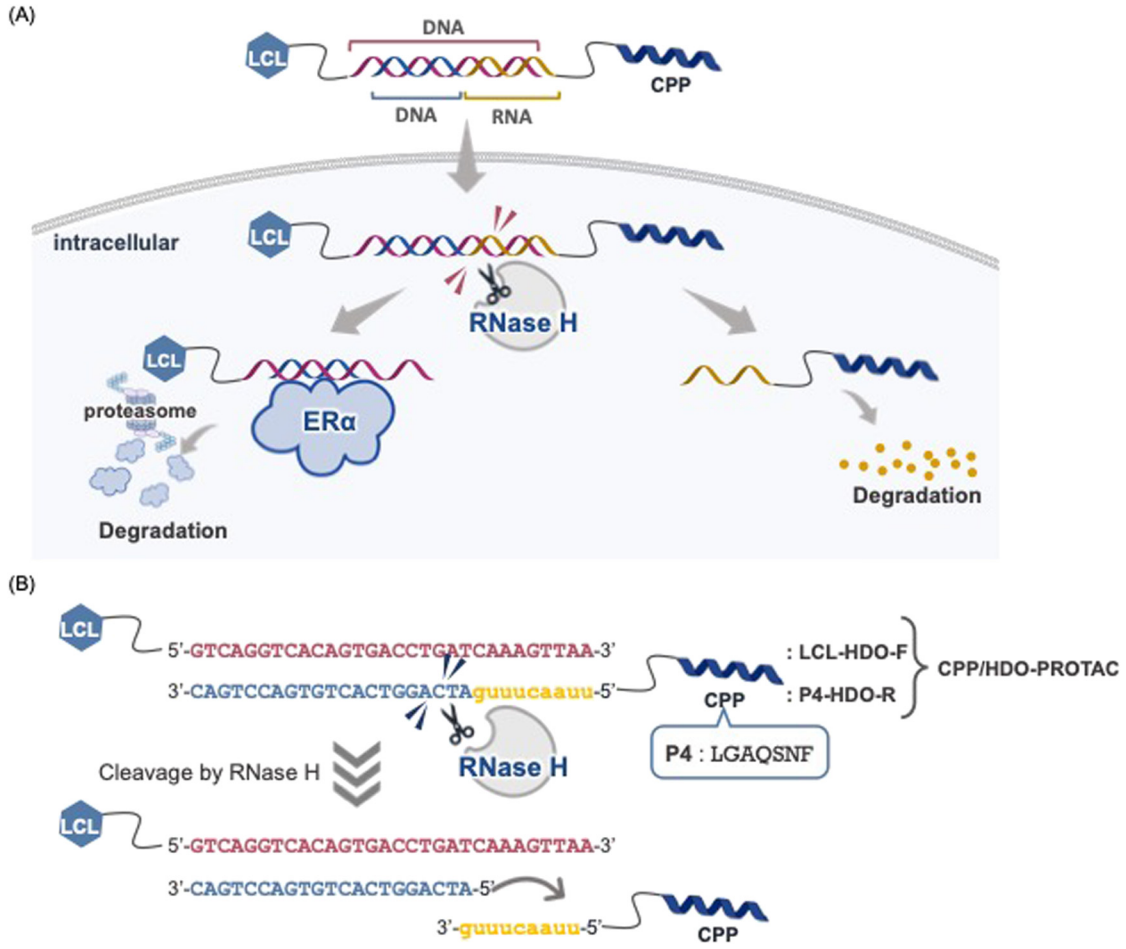

Fig. 1 (A) Schematic of the **CPP/HDO-PROTAC** responsible for degrading ERα. (B) Detailed sequence of the **CPP/HDO-PROTAC**.

 This journal is © The Royal Society of Chemistry 2024

hydrophobic residues to facilitate efficient conjugation and delivery. The study assessed the effectiveness of the **CPP/HDO-PROTAC** in RNase H-mediated cleavage, cellular uptake efficiency, ERα degradation activity and inhibition of cell proliferation.

2. Results and discussion

Based on the estrogen response element, a sequence for **ER(dec)** was extended by nine bases, and a sense strand with the sequence 5′-GTCAGGTCACAGTGACCTGATCAAAGTTAA-3′ was designed.[10,20] Additionally, an **HDO-F** modified with a hexynyl group at the 5′ end was created for this sequence.

LCL-HDO-F was synthesized by conjugating **HDO-F** and LCL161 (ref. 21) with an azidized PEG3 linker *via* a copper-catalyzed click reaction. In contrast, for the antisense strand, **HDO-R** was designed by modifying the 5′ end with a hexynyl group for the sequence containing nine bases of RNA (5′-uuaacuuugATCAGGTCACTGTGTGACCTGAC-3′). **HDO-R** was conjugated with the **P4** peptide *via* a copper-catalyzed click reaction to afford **P4-HDO-R** (Fig. 2 and Scheme 1). The synthesized **LCL-HDO-F** and **P4-HDO-R** were mixed and annealed by heating from room temperature to 95 °C and returning to room temperature to prepare **CPP/HDO-PROTAC**. In addition, an antisense strand **HDOdna-R** (5′-TTAACTTTGATCAGGTCACTGTGACCTGAC-3′) was designed as a negative control, in which all complementary strands of **HDO-F** were replaced with DNA sequences. **LCL-HDO-F** and **HDOdna-R** were annealed in a similar manner to generate **LCL-HDOdna**, and **LCL-HDOcl** was annealed with **HDO-F** to generate **ER(dec)-R** when the RNA strand was cleaved.

Published on 05 1403. Downloaded on 23/09/1404 10:43:09 ..

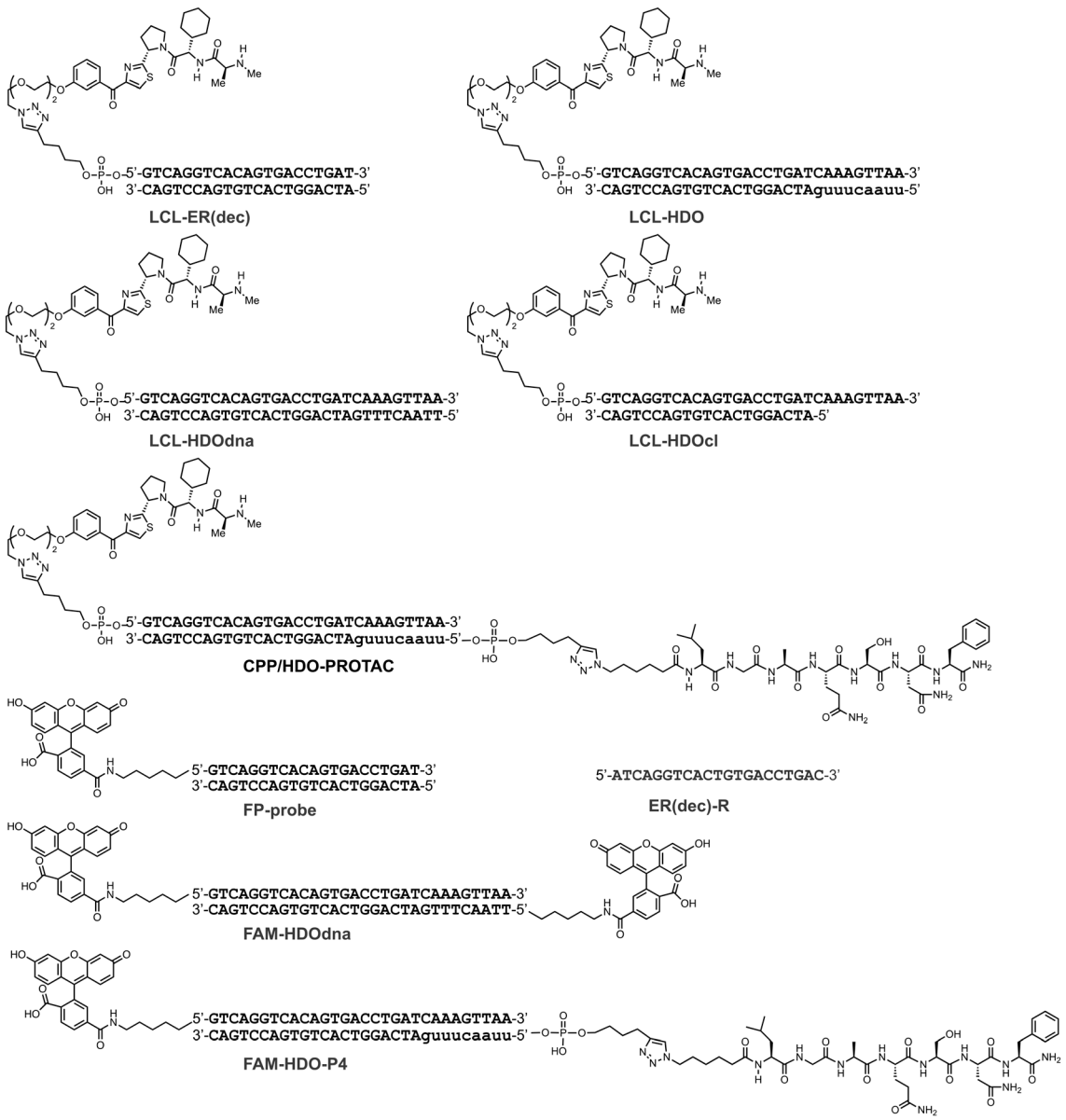

Fig. 2 Decoy-warheaded PROTACs and related molecules used in this study.

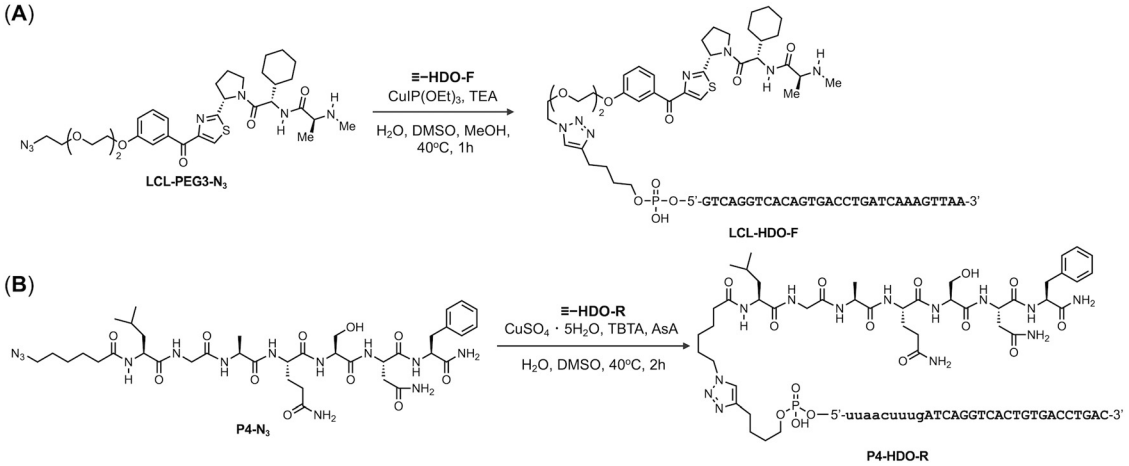

Scheme 1 Synthesis of (A) **LCL-HDO-F** and (B) **P4-HDO-R**.

Published on 05 1403. Downloaded on 23/09/1404 10:43:09 ..

The binding affinities of **LCL-ER(dec)**, **LCL-HDOcl**, **LCL-HDOdna** and **CPP/HDO-PROTAC** against ERα were evaluated by a competitive fluorescence polarization (FP) assay. For evaluation, compounds were added to a buffer system containing recombinant ERα and the **FP-probe**, a FAM-labeled **ER(dec)** at the 5′-end and 3′-end, and FP was measured (Fig. S5†).[10] The half inhibitory concentration (IC_{50}) values of the compounds were determined by calculating, which were 148 nM for **LCL-ER(dec)**, 24.6 nM for **LCL-HDOcl** and 1.2 nM for **LCL-HDOdna** (Table 1 and Fig. S5†). The increased binding affinity of **LCL-HDOcl** and **LCL-HDOdna** toward ERα may be attributed to additional interaction points provided by their longer nucleotide lengths. The **CPP/HDO-PROTAC** also exhibited an IC_{50} value of 3.0 nM, indicating that the binding activity is preserved even after conjugation with the **P4** peptide sequence.

The susceptibility of the HDO to RNase H-mediated cleavage was assessed by conducting experiments using a recombinant RNase H enzyme. After 2 h RNase H treatment, the decoys were analyzed using 20% denaturing polyacrylamide gel electrophoresis. The findings indicated that RNase H specifically degraded RNA in **CPP/HDO-PROTAC** and **LCL-HDO** with DNA–RNA heteroduplexes, leaving **LCL-HDO-F**, **HDO-R**, **LCL-HDOdna** and **ER(dec)-R** intact (Fig. 3). Therefore, it was hypothesized that **CPP/HDO-PROTAC** and **LCL-HDO**, upon cellular introduction, should be effectively targeted by RNase H, resulting in the degradation of the RNA component.

The ERα degradation activity of **CPP/HDO-PROTAC** was evaluated by western blotting in MCF-7 cells. **CPP/HDO-PROTAC** and a comparator, **LCL-HDOdna**, were added to cells, and the expression levels of ERα were evaluated after 24 h treatment. The results showed that **CPP/HDO-PROTAC** exhibited ERα degradation activity at 10 μM, suggesting that **CPP/HDO-PROTAC** penetrates cells and functions as a PROTAC without requiring transfection reagents (Fig. 4a). The ERα-degrading activity was also observed in the **LCL-ER(dec)** + **P4** co-treatment group at a concentration of 10 μM, even in the absence of transfection (Fig. 4b). At high concentrations, some of **LCL-ER(dec)** might have penetrated the cell membrane along with the hydrophobic CPP **P4** and been taken up into the cell. Conversely, ERα was not degraded when adding only **P4**, indicating **P4** does not enable ERα degradation (Fig. 4b). By contrast, **LCL-ER(dec)-P4**, which was directly conjugated with **P4** to **LCL-ER(dec)**, showed little ERα degrading activity (Fig. S6†).

High ERα expression, associated with poor prognosis and increased cell proliferation in breast cancer. Under transfection conditions, all PROTACs showed concentration-dependent inhibitory activity (Fig. S7†). In contrast, under non-transfection conditions, inhibitory activity was observed only for **CPP/HDO-PROTAC** (Fig. 5 and S8†). **LCL-ER(dec)** showed slight inhibitory activity at 10 μM, possibly because its sequence is shorter and its molecular weight is smaller than that of **LCL-HDOdna**, **LCL-HDO**, and **LCL-HDOcl**, therefore allowing partial cell penetration and activity at high concentrations. These results suggest that **CPP/HDO-PROTAC** was capable of efficiently entering cells and exerting its inhibitory effect even under non-transfection conditions, due to the presence of the **P4** sequence in CPP.

Intracellular transduction was observed using fluorescence microscopy with HDO-fluorescently labeled decoys; cells treated with **FAM-HDO-P4** exhibited brighter fluorescence than those treated with **FAM-HDOdna** (Fig. 6). After 2 h treatment with **FAM-HDO-P4**, fluorescence exhibited a point-like distribution and co-localized with the endosomal/lysosomal marker LysoTracker Red, indicating

Table 1 ERα binding affinity (IC_{50}) of **LCL-ER(dec)**, **LCL-HDOcl**, and **LCL-HDOdna**

Entry	Compound	IC_{50} (nM)
1	**LCL-ER(dec)**	148.0 ± 10.9
2	**LCL-HDOcl**	24.6 ± 3.93
3	**LCL-HDOdna**	1.2 ± 0.98
4	**CPP/HDO-PROTAC**	3.0 ±0.45

 This journal is © The Royal Society of Chemistry 2024

Published on 05 1403. Downloaded on 23/09/1404 10:43:09 ..

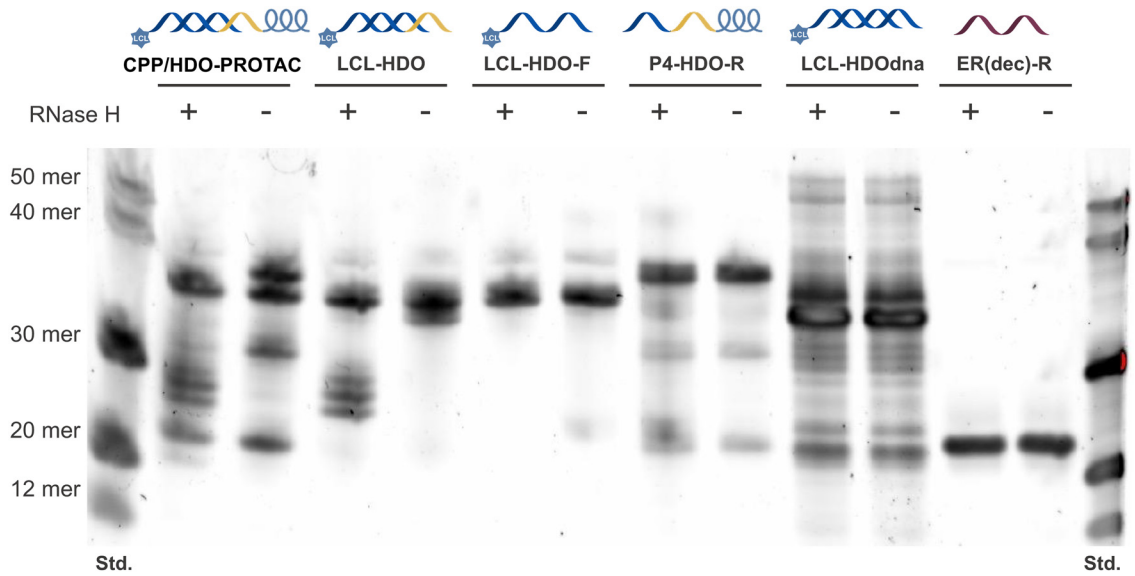

Fig. 3 Evaluation of HDO cleavage by RNase H. **CPP/HDO-PROTAC**, **LCL-HDO**, **LCL-HDO-F**, **P4-HDO-R**, **LCL-HDOdna** and **ER(dec)-R** were incubated with RNase H for 2 h. Full-length and digested oligonucleotides were resolved on 20% denaturing polyacrylamide gels.

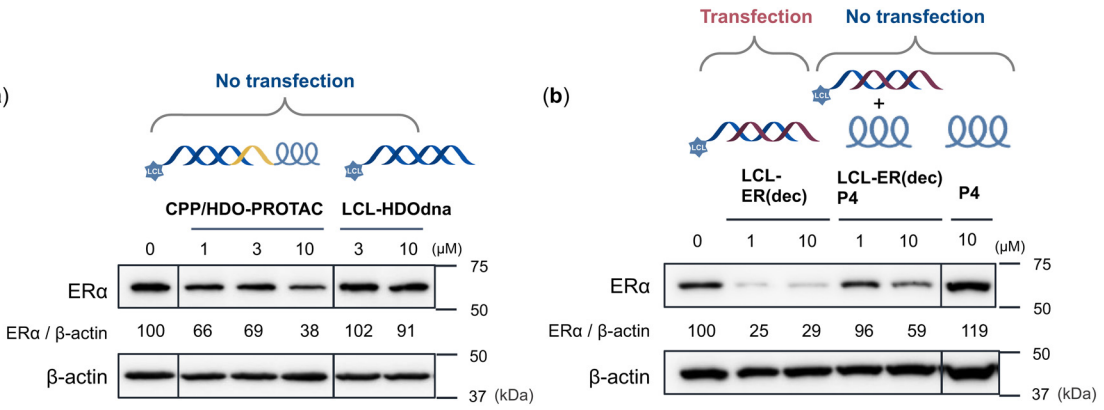

Fig. 4 Degradation of ERα by the synthesized PROTACs. Whole-cell lysates were analyzed by western blotting with the indicated antibodies (representative data are shown). The numbers below the ERα panels represent the ERα/β-actin ratios, normalized by designating the expression using the vehicle control (condition without a PROTAC) as 100%. (a) Degradation of ERα by **CPP/HDO-PROTAC**. MCF-7 cells were treated for 24 h with the indicated concentrations of **CPP/HDO-PROTAC** and **LCL-HDOdna**. (b) Degradation of ERα by **LCL-ER(dec)**. MCF-7 cells were transiently transfected for 24 h with the indicated concentrations of **LCL-ER(dec)**. An **LCL-ER(dec)** + **P4** mixture or **P4** alone was added to MCF-7 cells for 24 h.

that most internalized decoys remained within endosomes or lysosomes.

3. Conclusions

Decoy oligonucleotide-based PROTACs offer a novel strategy for targeting proteins where suitable small-molecule ligands are unavailable. Specifically, these PROTACs are highly promising for targeting TFs as their design leverages the motif sequences of TF DNA-binding domains. This method facilitates the development of PROTACs capable of targeting an extensive array of TFs. However, delivering all reported decoy oligonucleotide-based PROTACs into cells currently relies on transfection agents, highlighting the need for DDS technology integration to advance their pharmaceutical application. Furthermore, the use of native oligonucleotide-based decoy PROTACs face challenges related to chemical instability, necessitating substantial enhancement for their use in pharmaceutical applications. To address this issue, we developed **HDO-PROTAC**, adapting the HDO used for ASO delivery to decoy oligonucleotide-based PROTACs. We designed **CPP/HDO-PROTAC** based on the previously developed ERα-targeted lead sequence **LCL-ER(dec)**. **CPP/HDO-PROTAC** consists of **LCL-HDO-F** with LCL at the 5′ end of a 30-mer DNA and its complementary strand **P4-HDO-R**. **P4-HDO-R** was designed by extending the **ER(dec)-R** sequence with a 9-mer RNA and attaching the hydrophobic CPP **P4** to the 5′-end. Although general cationic CPPs have difficulty

Published on 05 1403. Downloaded on 23/09/1404 10:43:09 ..

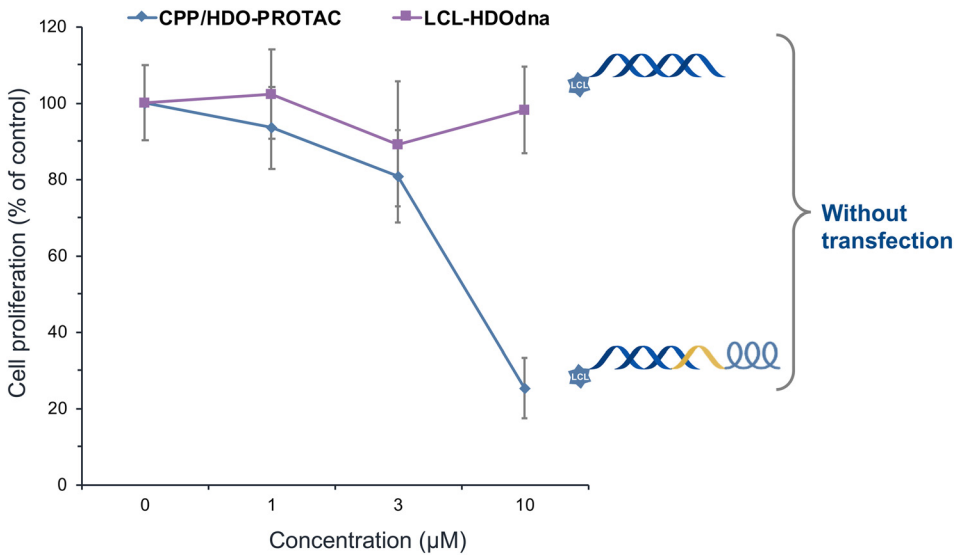

Fig. 5 Effects of **CPP/HDO-PROTAC** on the proliferation of ERα-positive breast cancer cells. Growth inhibition of ERα-positive breast cancer cells by **CPP/HDO-PROTAC**. MCF-7 cells were treated with 1–10 μM of **CPP/HDO-PROTAC** or **LCL-HDOdna** for 72 h, and cell proliferation was then evaluated using a cell viability assay. Data represent the mean ± standard deviation (n = 5).

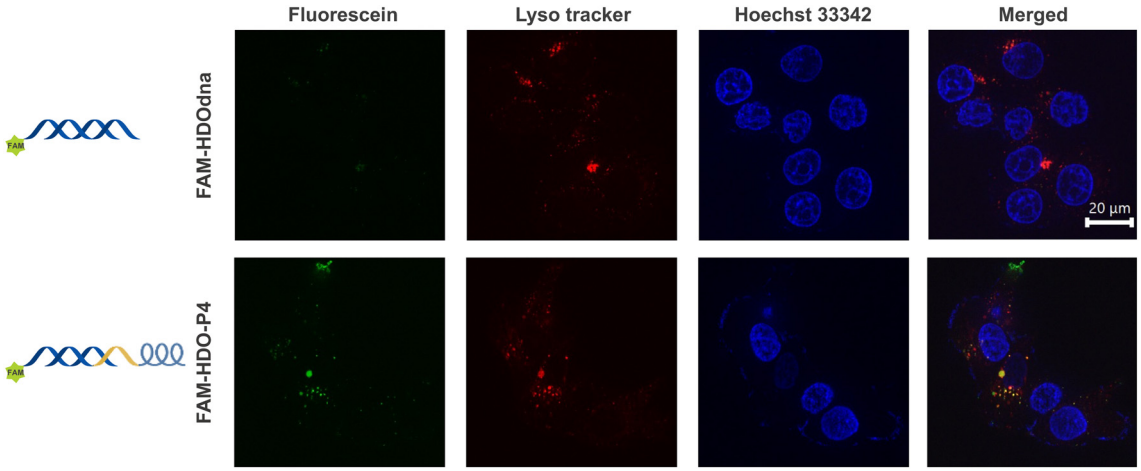

Fig. 6 Fluorescence microscopy images of MCF-7 cells treated with 10 μM decoy for 2 h. Nuclei and endosomes/lysosomes were stained by Hoechst 33342 and LysoTracker Red, respectively. The fluorescent microscopy observations were performed with a 100× objective lens. Scale bar: 20 μm.

conjugating with anionic nucleic acids, the **P4** used in this study is a hydrophobic peptide and its conjugates could be synthesized through a click reaction.

CPP/HDO-PROTAC has been proposed to be susceptible to RNase H-mediated degradation *in vitro*, but RNase H only cleaves double-stranded DNA and RNA and not other single or double strands. The binding activity of ERα by the assumed post-RNase H degradation product, **LCL-HDOcl**, and the control, **LCL-HDOdna**, demonstrated enhanced binding compared with **LCL-ER(dec)**. Evaluation of the ERα degradation activity of **CPP/HDO-PROTAC** revealed that **CPP/HDO-PROTAC** was effective at a concentration of 10 μM. Furthermore, the ability of **CPP/HDO-PROTAC** to inhibit MCF-7 cell proliferation indicates it may suppress estrogen signaling. This study confirms that intracellular delivery of decoy oligonucleotide-based PROTACs is possible by combining the hydrophobic CPP **P4** with an HDO, allowing for the first time the transfection-independent introduction of PROTACs into cells. Improving transport efficiency and tissue specificity is vital for unlocking the therapeutic potential of these PROTACs. The introduction of artificial nucleic acids that increase the chemical stability of the RNA strand is expected to improve its stability after intracellular transport. Continued efforts in DDS optimization are essential for their successful clinical application.

4. Experimental section

General chemistry methods

All chemicals were purchased from Sigma-Aldrich, FUJIFILM Wako Pure Chemicals, and Tokyo Chemical Industry, and

 This journal is © The Royal Society of Chemistry 2024

Published on 05 1403. Downloaded on 23/09/1404 10:43:09 ..

were used without further purification. High-resolution mass spectra were measured using a Shimadzu IT-TOF MS equipped with an electrospray ionization source.

Oligonucleotide synthesis

Decoys were synthesized on a 1.0 μmol scale using an automated DNA synthesizer (T-Series, Nihon Techno Service) by means of phosphoramidite chemistry with 5′-dimethoxytrityl-2′-deoxynucleoside phosphoramidites (Glen Research). To synthesize a sequence containing a hexynyl group at the 5′ end, synthesis continued according to the standard protocol and 5′-hexynyl phosphoramidite (Glen Research) was used in the last coupling step to introduce a hexynyl group at the 5′-terminus. To synthesize fluorescein-labeled oligonucleotides, synthesis continued according to the standard protocol and 6-Fluorescein phosphoramidite (Sigma-Aldrich) was used in the last coupling step to introduce FAM dye at the 5′-terminus. DNA on solid support (CPG) were treated with 28% ammonium hydroxide for 15 h at 55 °C and concentrated *in vacuo*. RNA Deprotected decoys were purified using reverse phase HPLC. HPLC conditions were as follows; column: CAPCELL PAK MG-II (C18, 10 × 250 mm, 5 μm; OSAKA soda), mobile phase: *A* = 0.1 M triethylammonium acetate (TEAA) buffer (pH 7.0), B = CH_3-CN. Gradient: *B*% = 10–40 over 20 min, 40–100 over 5 min. Flow rate: 1 mL min^{-1}, detection: 260 nm, column temperature: 35 °C. Concentration of the solution of decoys was determined using NanoDrop OneC (Thermo Fisher Scientific) by absorbance at 260 nm and molar absorbance coefficient (ε_{260}) calculated from OligoAnalyzer (IDT).

Peptide synthesis

The peptides were synthesized by Fmoc-based solid-phase methods. A representative coupling and deprotection cycle are described as follows. Rink Amide ChemMatrix resin was soaked for 30 min in CH_2Cl_2. After the resin had been washed with DMF, the Fmoc protecting group was removed by treatment with 25% piperidine in DMF for 15 min at room temperature. Amino acids were coupled for 1 hour using 4 equiv. of Fmoc-protected amino acid, 4 equiv. of (1-cyano-2-ethoxy-2-oxoethylidenaminooxy)dimethylamino-morpholinocarbenium hexafluorophosphate (COMU) as the activating agent, and 8 equiv. of diisopropylethylamine (DIPEA) in NMP.

The peptide was suspended in cleavage cocktail (95% TFA, 2.5% water, 2.5% triisopropylsilane) at 42 °C for 30 min on Razor (CEM corp.) to cleave from the resin. TFA was evaporated to a small volume under a stream of N_2 and dripped into cold ether to precipitate the peptide. The peptides were dissolved in dimethyl sulfoxide and purified using reverse-phase HPLC (Waters) using a Discovery® BIO Wide Pore C18 column (Supelco, Bellefonte, PA, USA) (25 cm × 21.2 mm solvent A: 0.1% TFA/water, solvent B: 0.1% TFA/CH_3CN, flow rate: 10.0 mL min^{-1}, gradient: 10–90% gradient of solvent B over 40 min). After purification, the peptide solutions were lyophilized, and peptide purity was assessed using UPLC (Waters) and a ACQUITY UPLC® BEH C18 1.7 μm column (2.1 × 50 mm; solvent A: 0.1% TFA/water, solvent B: 0.1% TFA/CH_3CN, flow rate: 0.5 mL min^{-1}, gradient: 10–90% gradient of solvent B over 4 min).

Synthesis of chimeric molecules by click reaction

To a solution of IAP ligand (**LCL-PEG3-N_3**) in MeOH (10 mM, 168 μL, 1.68 μmol) was added the ERα-binding decoy **5′-hexynyl-HDO-F** in H_2O (1.6 mM, 500 μL, 0.8 μmol), TEA in DMSO (32 mM, 250 μL, 8 μmol), and $CuIP(OEt)_3$ in DMSO (35.8 mM, 250 μL, 11.2 μmol). The mixture was incubated at 40 °C for 3 h. The reaction mixture was purified using HPLC and lyophilized. The collected oligo was precipitated in a solution of 0.3 M sodium acetate (pH 5.2)/70% ethanol to give the single strand of **LCL-HDO-F**, which was resuspended in nuclease-free water to prepare a stock solution (1 mM, 232 μL, 0.232 μmol, 29%).

To a solution of decoys in water and DMSO (7 : 3) were added an azide-peptide (3 equiv.), $CuSO_4$ (10 equiv.), sodium ascorbate (5 equiv.), and tris[(1-benzyl-1*H*-1,2,3-triazol-4-yl) methyl]amine (10 equiv.). The mixture was incubated at 45 °C for 2 h. The reaction mixture was purified using HPLC and lyophilized. The collected oligo was precipitated in a solution of 0.3 M sodium acetate (pH 5.2)/70% ethanol to give the single strand of **P4-HDO-R**, which was resuspended in nuclease-free water to prepare a stock solution.

Finally, **LCL-HDO-F** and the corresponding antisense strand (**P4-HDO-R**) was mixed in an aqueous solution and hybridized by heating at 95 °C for 10 min and gradually returning to room temperature to give the double-stranded title compound **CPP/HDO-PROTAC**.

Fluorescence polarization assay. Binding of test compounds to human ERα protein was measured using a fluorescence polarization assay (Invitrogen's protocol) containing recombinant ERα full-length protein (Invitrogen) and TE buffer (10 mM Tris-HCl, 1 mM EDTA, pH 7.5). ERα and fluorescein-labeled **FP-probe** were diluted with assay buffer to final concentrations of 100 nM and 0.05 nM, respectively, and 25 μL of the diluted solution was added to each well black low-volume assay plate (Greiner). Then, 25 μL of TE buffer containing the test substance was added to each well. After incubation at room temperature for 30 min, the fluorescence polarization signal (mP value) was measured using a plate reader equipped with 480 nm excitation/635 nm emission filter (EnVision 2105, Perkin Elmer). The data represent means S.D. (n = 3).

Enzyme tolerance evaluation (dPAGE). Denaturing PAGE (dPAGE) experiments were conducted using a 20% polyacrylamide gel (8 cm × 9 cm) containing 7 M urea. Electrophoresis was performed at a constant pressure of 200 V for 30 min. The gels were stained with a diluted solution of SYBR Green I dye in distilled water. For the cleavage of decoys by exonuclease III, a solution consisting of 1 × NE buffer, 1 μM sample, and 4 units of exonuclease III (NEW

Published on 05 1403. Downloaded on 23/09/1404 10:43:09 ..

ENGLAND BioLabs, M0206S) was incubated at 37 °C for 2 h. Subsequently, 12 mM EDTA was added to the solution, and the reaction was quenched by further incubation at 70 °C for 30 min. The above mixture (4 μL) was mixed with loading buffer (80% formamide, 20% TE buffer, 4 μL), and heated at 95 °C for 5 minutes. The resulting mixture was analyzed by dPAGE. Finally, the gels were imaged with UV illumination with the ChemiDoc Touch Imaging System (Bio-Rad).

Cell culture and transfection. Human breast carcinoma MCF-7 cells were purchased from ATCC (Manassas, VA), and maintained in RPMI 1640 medium (Sigma-Aldrich, St. Louis, MO, USA) containing 10% fetal bovine serum (FBS) and 100 U mL^{-1} penicillin, 100 μg mL^{-1} streptomycin (NACALAI TESQUE). To transfect the synthesized decoys, MCF-7 cells were seeded in 6-well plates at a density of 3.0×10^5 cells per well and cultured at 37 °C with atmosphere of 5% CO_2. After 24 hours, the cells were transfected with Lipofectamine 2000 reagent (Thermo Fisher Scientific, Waltham, MA, USA) as follows. 125 μL of Opti-MEM I reduced-serum medium (Gibco) with various concentrations of decoys were mixed with 125 μL of Opti-MEM with 4.5 μL of Lipofectamine 2000 (Invitrogen) and incubated at room temperature for 10 min. A total of 250 μL of the mixture was dropped into the culture wells and further incubated. After 24 h of incubation, cells were harvested and subjected to western blot analysis.

Western blot assay. Cells were washed with phosphate buffer (PBS) and lysed with SDS lysis buffer (0.1 M Tris-HCl, pH 7.4, 10% glycerol, 1% SDS) and immediately boiled for 10 min to obtain clear lysates. The protein concentration was measured by the BCA method (Thermo Fisher Scientific), and the lysates containing equal amounts of proteins were separated by SDS-PAGE and transferred to PVDF membranes (Merck Millipore Ltd.) for western blotting analysis using the appropriate antibodies. The immunoreactive proteins were visualized using the Clarity Western ECL substrate (Bio-Rad), and light emission intensity was quantified with a ChemiDoc™ MP with Image Lab Software version 6.0.1 (Bio-Rad). The antibodies used in this study were anti-ERα antibody (Cell Signaling Technology, Danvers, MA USA; 8644), and anti-β-actin antibody (Sigma-Aldrich, A2228).

Cell proliferation assay. MCF-7 cells were seeded in 96-well plates at a density of 5.0×10^3 cells per well and cultured for 24 h at 37 °C with atmosphere of 5% CO_2. Then, the cells were transfected with various concentrations of decoys and Lipofectamine 2000, and cultured for 72 hours. Cell viability was determined using water-soluble tetrazolium WST-8 (4-[3-(2-methoxy-4-nitrophenyl)-2-(4-nitrophenyl)-2*H*-5-tetrazolio]-1,3-benzene disulfonate) for the spectrophotometric assay according to the manufacturer's instructions (Dojindo). Cells treated with compounds were incubated with WST-8 reagent for 1 h at 37 °C in a humidified atmosphere of 5% CO_2. The absorbance at 450 nm of the medium was measured using an Multiskan FC (Thermo Fisher Scientific).

Fluorescence microscopy. MCF-7 cells were seeded onto 35 mm glass bottom dish (2000 cells per well) and incubated overnight in 2 mL of RPMI1640 containing 10% FBS. The medium was then replaced with fresh medium containing 10% FBS, and decoys was applied to well at a concentration of 10 μM. After 2 h incubation at 37 °C, the medium was removed, and the cells were washed 3 times with PBS. The intracellular distribution of each decoy was observed by fluorescence microscopy after staining late endosomes/lysosomes with LysoTracker Red DND-99 and nuclei with Hoechst 33342. Fluorescence microscopy was performed using a BZ-X810 (Keyence, Osaka, Japan) equipped with a 100× objective lens, and further sectioning was performed to acquire images.

Abbreviations

PROTAC	Proteolysis targeting chimera
IAP	Inhibitor of apoptosis protein
TF	Transcription factor
ERα	Estrogen receptor α
FAM	Fluorescein
DDS	Drug delivery systems
CPP	Cell-penetrating peptide
TEA	Triethylamine
DMF	*N*,*N*-Dimethylformamide

Data availability

Raw data were generated at National Institute of Health Sciences. Derived data supporting the findings of this study are available from the corresponding author Y. D. on request.

Author contributions

M. N., N. O., M. H., D. W., and G. T. performed the experiments and analyzed results. M. N., N. O., T. I., and Y. D. designed the research and wrote the paper. All authors discussed the results and commented on the manuscript.

Conflicts of interest

There is no conflict of interest to declare.

Acknowledgements

This study was supported in part by grants from AMED under grant numbers 24mk0121286, 24ama221127, and 24ak0101185 (all to Y. D.); 24ak0101186 (to T. I. and N. O.); 24fk0310504 (to N. O.). The study also received support from the Japan Society for the Promotion of Science (KAKENHI, grants 21K05320 and 23H04926, both to Y. D.; 18K06567 and 21K06490, both to N. O.) and JSPS Fellows 21J23036 to Miyako Naganuma. We thank Edanz (**https://www.jp.edanz.com/ac**) for editing a draft of this manuscript.

 This journal is © The Royal Society of Chemistry 2024

Published on 05 1403. Downloaded on 23/09/1404 10:43:09 ..

References

1 K. Li and C. M. Crews, PROTACs: past, present and future, *Chem. Soc. Rev.*, 2022, **51**(12), 5214–5236, DOI: **10.1039/D2CS00193D**.

2 W. Wang, S. He, G. Dong and C. Sheng, Nucleic-Acid-Based Targeted Degradation in Drug Discovery, *J. Med. Chem.*, 2022, **65**(15), 10217–10232, DOI: **10.1021/acs.jmedchem.2c00875**.

3 Y. Liu, X. Qian, C. Ran, L. Li, T. Fu, D. Su, S. Xie and W. Tan, Aptamer-Based Targeted Protein Degradation, *ACS Nano*, 2023, **17**(7), 6150–6164, DOI: **10.1021/acsnano.2c10379**.

4 J. Liu, H. Chen, H. U. Kaniskan, L. Xie, X. Chen, J. Jin and W. Y. Wei, TF-PROTACs Enable Targeted Degradation of Transcription Factors, *J. Am. Chem. Soc.*, 2021, **143**(23), 8902–8910, DOI: **10.1021/jacs.1c03852**.

5 Y. Yan, J. Shao, D. Ding, Y. Pan, P. Tran, W. Yan, Z. Wang, H. Y. Li and H. Huang, 3-Aminophthalic acid, a new cereblon ligand for targeted protein degradation by O'PROTAC, *Chem. Commun.*, 2022, **58**(14), 2383–2386, DOI: **10.1039/d1cc06525d**.

6 L. Zhang, L. Li, X. Wang, H. Liu, Y. Zhang, T. Xie, H. Zhang, X. Li, T. Peng and X. Sun, *et al.*, Development of a novel PROTAC using the nucleic acid aptamer as a targeting ligand for tumor selective degradation of nucleolin, *Mol. Ther. – Nucleic Acids*, 2022, **30**, 66–79, DOI: **10.1016/j.omtn.2022.09.008**.

7 H. Tsujimura, M. Naganuma, N. Ohoka, T. Inoue, M. Naito, G. Tsuji and Y. Demizu, Development of DNA Aptamer-Based PROTACs That Degrade the Estrogen Receptor, *ACS Med. Chem. Lett.*, 2023, **14**(6), 827–832, DOI: **10.1021/acsmedchemlett.3c00126**.

8 Y. Wang, G. Yang, X. Zhang, R. Bai, D. Yuan, D. Gao, Q. He, Y. Yuan, X. Zhang and J. Kou, *et al.*, Antitumor Effect of Anti-c-Myc Aptamer-Based PROTAC for Degradation of the c-Myc Protein, *Adv. Sci.*, 2024, **11**(26), e2309639, DOI: **10.1002/advs.202309639**.

9 L. Kong, F. Meng, P. Zhou, R. Ge, X. Geng, Z. Yang, G. Li, L. Zhang, J. Wang and J. Ma, *et al.*, An engineered DNA aptamer-based PROTAC for precise therapy of p53-R175H hotspot mutant-driven cancer, *Sci. Bull.*, 2024, **69**(13), 2122–2135, DOI: **10.1016/j.scib.2024.05.017**.

10 M. Naganuma, N. Ohoka, G. Tsuji, H. Tsujimura, K. Matsuno, T. Inoue, M. Naito and Y. Demizu, Development of Chimeric Molecules That Degrade the Estrogen Receptor Using Decoy Oligonucleotide Ligands, *ACS Med. Chem. Lett.*, 2022, **13**(1), 134–139, DOI: **10.1021/acsmedchemlett.1c00629**.

11 M. Naganuma, N. Ohoka, G. Tsuji, T. Inoue, M. Naito and Y. Demizu, Structural Optimization of Decoy Oligonucleotide-Based PROTAC That Degrades the Estrogen Receptor, *Bioconjugate Chem.*, 2023, **34**(10), 1780–1788, DOI: **10.1021/acs.bioconjchem.3c00332**.

12 K. Nishina, W. Piao, K. Yoshida-Tanaka, Y. Sujino, T. Nishina, T. Yamamoto, K. Nitta, K. Yoshioka, H. Kuwahara and H. Yasuhara, *et al.*, DNA/RNA heteroduplex oligonucleotide for highly efficient gene silencing, *Nat. Commun.*, 2015, **6**, 7969, DOI: **10.1038/ncomms8969**.

13 S. M. Hammond, A. Aartsma-Rus, S. Alves, S. E. Borgos, R. A. M. Buijsen, R. W. J. Collin, G. Covello, M. A. Denti, L. R. Desviat and L. Echevarria, *et al.*, Delivery of oligonucleotide-based therapeutics: challenges and opportunities, *EMBO Mol. Med.*, 2021, **13**(4), e13243, DOI: **10.15252/emmm.202013243**.

14 M. Jayaraman, S. M. Ansell, B. L. Mui, Y. K. Tam, J. Chen, X. Du, D. Butler, L. Eltepu, S. Matsuda and J. K. Narayanannair, *et al.*, Maximizing the potency of siRNA lipid nanoparticles for hepatic gene silencing in vivo, *Angew. Chem., Int. Ed.*, 2012, **51**(34), 8529–8533, DOI: **10.1002/anie.201203263**.

15 H. Kaburagi, T. Nagata, M. Enomoto, T. Hirai, M. Ohyagi, K. Ihara, K. Yoshida-Tanaka, S. Ebihara, K. Asada and H. Yokoyama, *et al.*, Systemic DNA/RNA heteroduplex oligonucleotide administration for regulating the gene expression of dorsal root ganglion and sciatic nerve, *Mol. Ther. – Nucleic Acids*, 2022, **28**, 910–919, DOI: **10.1016/j.omtn.2022.05.006**.

16 S. M. Jirka, H. Heemskerk, C. L. Tanganyika-de Winter, D. Muilwijk, K. H. Pang, P. C. de Visser, A. Janson, T. G. Karnaoukh, R. Vermue and P. A. t Hoen, *et al.*, Peptide conjugation of 2′-O-methyl phosphorothioate antisense oligonucleotides enhances cardiac uptake and exon skipping in mdx mice, *Nucleic Acid Ther.*, 2014, **24**(1), 25–36, DOI: **10.1089/nat.2013.0448**.

17 A. Gonzalez-Barriga, B. Nillessen, J. Kranzen, I. D. G. van Kessel, H. J. E. Croes, B. Aguilera, P. C. de Visser, N. A. Datson, S. A. M. Mulders and J. C. T. van Deutekom, *et al.*, Intracellular Distribution and Nuclear Activity of Antisense Oligonucleotides After Unassisted Uptake in Myoblasts and Differentiated Myotubes In Vitro, *Nucleic Acid Ther.*, 2017, **27**(3), 144–158, DOI: **10.1089/nat.2016.0641**.

18 D. Honcharenko, K. Druceikaite, M. Honcharenko, M. Bollmark, U. Tedebark and R. Stromberg, New Alkyne and Amine Linkers for Versatile Multiple Conjugation of Oligonucleotides, *ACS Omega*, 2021, **6**(1), 579–593, DOI: **10.1021/acsomega.0c05075**.

19 S. M. G. Jirka, P. A. C. t Hoen, V. Diaz Parillas, C. L. Tanganyika-de Winter, R. C. Verheul, B. Aguilera, P. C. de Visser and A. M. Aartsma-Rus, Cyclic Peptides to Improve Delivery and Exon Skipping of Antisense Oligonucleotides in a Mouse Model for Duchenne Muscular Dystrophy, *Mol. Ther.*, 2018, **26**(1), 132–147, DOI: **10.1016/j.ymthe.2017.10.004**.

20 V. Kumar and P. Chambon, The Estrogen-Receptor Binds Tightly To Its Responsive Element As A Ligand-Induced Homodimer, *Cell*, 1988, **55**(1), 145–156, DOI: **10.1016/0092-8674(88)90017-7**.

21 N. Ohoka, K. Okuhira, M. Ito, K. Nagai, N. Shibata, T. Hattori, O. Ujikawa, K. Shimokawa, O. Sano and R. Koyama, *et al.*, In Vivo Knockdown of Pathogenic Proteins via Specific and Nongenetic Inhibitor of Apoptosis Protein (IAP)-dependent Protein Erasers (SNIPERs), *J. Biol. Chem.*, 2017, **292**(11), 4556–4570, DOI: **10.1074/jbc.M116.768853**.